# Mechanisms for the formation of $H_2$ and $O_2$ from x-ray irradiated dense ice

Yunfeng Liang and John S. Tse
*Department of Physics and Engineering Physics, University of Saskatchewan, Saskatoon, Canada S7N 5E2*
(Received 2 January 2009; published 11 March 2009)

Recent experiment [W. L. Mao *et al.*, Science **314**, 636 (2006)] has shown that when ice VII is irradiated by intense x ray it dissociates into an alloy of $O_2$ and $H_2$ at high pressure. It is proposed here that irradiation stimulates the creation of "excess" electrons and holes, as well as radical defects, which interact with each other to promote the dissociation. First-principles calculations on ice VII show that $H_2O$ dissociates into $H^{\cdot}$ and $OH^{\cdot}$ within 100 fs after core ionization. Secondary interaction of $H^{\cdot}$ with an excess electron leads to the formation of an interstitial $H_2$ molecule. On the other hand, $H_2O_2$, a precursor of $O_2$, is formed when an $OH^{\cdot}$ radical is in an electron-deficient environment. Direct formation of a nearly free $O_2$ is observed in a model consisting of two adjacent $OH^{\cdot}$ in a highly electron-deficient environment. The theoretical results offer an atomistic insight to rationalize the pressure effect on the dissociation of water to $O_2$ and $H_2$.

DOI: 10.1103/PhysRevB.79.104105 PACS number(s): 71.15.Pd

## I. INTRODUCTION

The physical and chemical properties of ice are of fundamental importance in many fields of science.[1] Water under compression transforms into high-density ice VII,[2] where the water is still in the molecular form.[3–5] At extreme pressure, ice VII has shown to exhibit a variety of exotic behaviors such as hydrogen bond symmetrization[6–8] and superionic conductivity.[9,10] Therefore the study of ice VII has attracted extensive interests.[6–11] Recently, Mao *et al.*[12] reported that ice VII decomposes into a molecular alloy of $O_2$ and $H_2$ when exposed to intense x ray. Pickard and Needs[13] have attempted to identify the structure of the alloy using a random structural search strategy with first-principles density-functional calculations. However, the dissociation mechanism is still unknown.

Water radiolysis is a complex process involving a large number of competing reactions.[14] It is not feasible to simulate all the complex processes associated with the temporal evolution of the photoionized structure. However, it is well known that the primary species, detected after the interaction of x ray with water, are $H^{\cdot}$ and $OH^{\cdot}$ radicals.[14–17] Under ambient pressure no substantial amount of $H_2$ and $O_2$ has been reported in bulk ice and water irradiated by x ray.[15] This would suggest that pressure may facilitate the formation of these molecules. A soft x-ray irradiation experiment on ice using photon energy ~3–900 eV (Ref. 15) has shown that radiation induced processes are dominated by the interaction of the water with secondary (Auger) electrons produced after photoionization. On the other hand, holes can be formed in the valence band when the ionized core is screened by the cascade of a valence electron. These "excess" electrons and holes delocalize within the ice sample,[15,18] travel more than 120 Å within 10 fs,[19] and help to induce secondary electronic processes. The mobility of the electrons and holes is expected to be sensitive to the energy barrier which can be altered substantially by pressure. A likely scenario for the formation of $H_2$ and $O_2$ is through the interactions of the electrons or holes with radical defects.[20,21] First-principles calculations[22–24] have demonstrated the importance of interactions between defects and excess electrons in H-bonded materials. In particular, the formation of $H_2$ in hydrogen-bonded $KH_2PO_4$ (KDP) (Ref. 24) has been shown to be assisted by electrons or holes. To investigate possible interactions between radical defects with electrons or holes in irradiated ice VII, *ab initio* Car-Parrinello molecular-dynamics (CPMD) calculations[25] in the canonical ensemble (NVT) and microcanonical ensemble (NVE) were performed on model systems.

The paper is organized as follows. In Sec. II details on the defect models and the computational methods will be given. Results of the calculations and the role of pressure in the dissociation mechanisms will be presented and discussed in Sec. III.

## II. COMPUTATIONAL METHODS

The defect models are created as follows. The initial proton-disordered ice VII structure with a zero net dipole moment, which consists of 16 $H_2O$ f.u., was taken from the work of Kuo and Klein.[26] To generate models with a single $OH^{\cdot}$ defect, a H atom along one of the four O···O directions was removed. To construct structural models with a $H^{\cdot}$ defect, a H atom is placed between oxygen atoms in one of the three O···O directions (1, −1, −1), (−1, 1, 1), and (−1, −1, −1) as shown in Fig. 1. To distinguish the different models, a D defect is referred to a H atom placed along the (1, −1, −1) direction; a $NH_3$-like defect is referred to a H atom placed along the (−1, 1, 1) direction; and an in-plane defect is referred to a H atom put along the (−1, −1, −1) direction. The initial distance between the H defect and the oxygen atom in these models was chosen to be the same as a normal O-H bond (0.98 Å). For each model, CPMD calculations were performed at 300 K and a constant volume (at a pressure ~3 GPa) and the temperature was controlled by means of a Nosé thermostat.[27] The trajectories from at least 24 000 molecular-dynamics (MD) steps (~3 ps) were then analyzed. In some cases, additional calculations of 3–5 ps were performed to obtain the vibrational frequencies and to estimate the lifetime of specific species of interest. All calculations were performed with the QUANTUM ESPRESSO package.[28] Troullier-Martins pseudopotentials (PPs) (Ref.

 

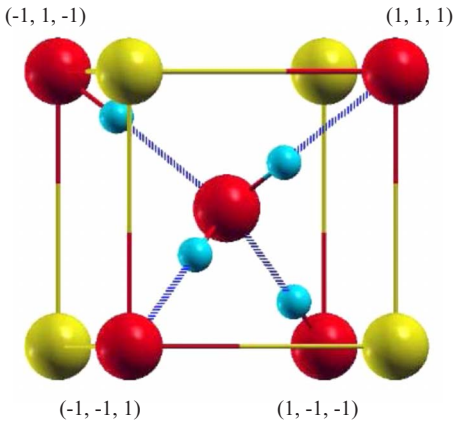


FIG. 1. (Color online) A model for generating H defects in ice VII. The oxygen atoms are arranged in a bcc lattice. Hydrogen atoms (in blue) are placed along (1,1,1), (−1, −1, 1), (−1, 1, −1) and (1, −1, −1) (O atom in red). Defect models are built as described in the text.

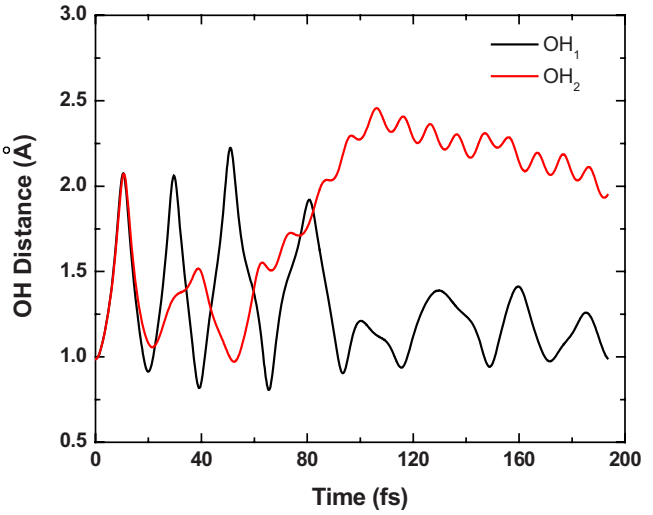


FIG. 2. (Color online) The initial dissociation process after core ionization: $H_2O$ dissociates into H and OH radicals in 100 fs.

29) were used to describe valence electron-nuclei interactions. Electronic orbitals were expanded in a plane-wave basis set using an energy cutoff of 80 Ry. The Becke-Lee-Yang-Parr (BLYP) functional[30] was used in most calculations. The Perdew-Burke-Ernzerhof (PBE) functional[31] was used to check the reliability of the BLYP functional and in the construction of PPs with a core hole on the oxygen atom. A fictitious electron mass of 200 a.u. and a time step of 5 a.u. were used for the integration of the ionic motions.[25] Brillouin zone sampling was restricted to the Γ point.

An electronic excitation occurs when the energy of the incident photon (e.g., ~9 KeV) is sufficient to promote an electron from a core state to an unoccupied state. Once the electron is ejected, it will leave a deep potential well in the core state (core hole) of the absorbing atom. Electrons within the system will respond to the new potential and migrate towards and screen the core hole to form core-valence excitations or core ionization states. This can be simulated by the generation of an excited pseudopotential by removing a single electron from the core.[28] In a previous study of the x-ray absorption spectra of ice and liquid water, a similar full core hole pseudopotential augmented by a "screening" electron in the valence band was used with success.[32] A similar treatment of the core hole has also been used in the study of ultrafast molecular dissociation of water in ice.[17]

## III. RESULTS AND DISCUSSIONS

### A. Validation of the model

We first examine the effect of photoionization in ice VII. Two sets of calculations were performed. The first calculation was intended to mimic the response of the system to core ionization. In this case, the pseudopotential of a randomly selected O atom in the model ice VII structure is replaced by a PP generated with one 1*s* electron removed. The second calculation was concerned with the effect of core-valence excitation. Once again an O atom was chosen randomly and the PP is replaced by a core-ionized PP, but an additional electron is put back into the conduction band. In both cases, in excellent agreement with experiments,[16] it is found that $H_2O$ dissociates into $H^{\cdot}$ and $OH^{\cdot}$ radicals within 100 fs (Fig. 2). In the ensuing discussion secondary processes between defects with electrons and holes in the valence band that might lead to the formation of $H_2$ and $O_2$ are explored.

### B. Formation of $H_2$

First, interactions of a $H^{\cdot}$ defect at the presence and absence of electrons or holes in the valence band were investigated. CPMD calculations show that under a neutral or electron-deficient (hole) environment all three H-defect models failed to produce any molecular $H_2$. However, at the presence of an electron the $NH_3$-like defect model produced a $H_2$ molecule almost instantaneously. This is confirmed by the short H-H contact of 0.76 Å in the H-H radial distribution function (RDF) (Fig. 3) which is close to 0.74 Å of the free molecule.[33] When compared to neutral and electron-deficient environments, the H-H distribution in the 2–3 Å range shifted to shorter H-H distances and becomes broader indicating that the proton is disordered. The formation of $H_2$ was also observed in models with D and in-plane defects. Analysis of MD trajectories reveals that a nascent "$H_2$" is formed in the vicinity of an $OH^{\cdot}$ radical (inset of Fig. 3). The vibrational frequencies of the $H_2$ found in all three defect models were calculated from the Fourier transform of the respective velocity autocorrelation function from simulations using NVE ensemble. H-H stretch bands (shown in Fig. 4) calculated at 4289, 4327, and 4404 $cm^{-1}$ for the D defect, $NH_3$-like, and in-plane models, respectively, are close to the calculated 4302 $cm^{-1}$ and observed 4161 $cm^{-1}$ for a free $H_2$ molecule. Since all three types of defects can coexist and the H-H vibron of the $NH_3$-like defect is very close to that of the in-plane defect, superposition of the three power spectra yields two peaks. This is consistent with the doublet observed in the Raman spectrum.[12] The calculated splitting of 115 $cm^{-1}$ between D and in-plane defects may be compared

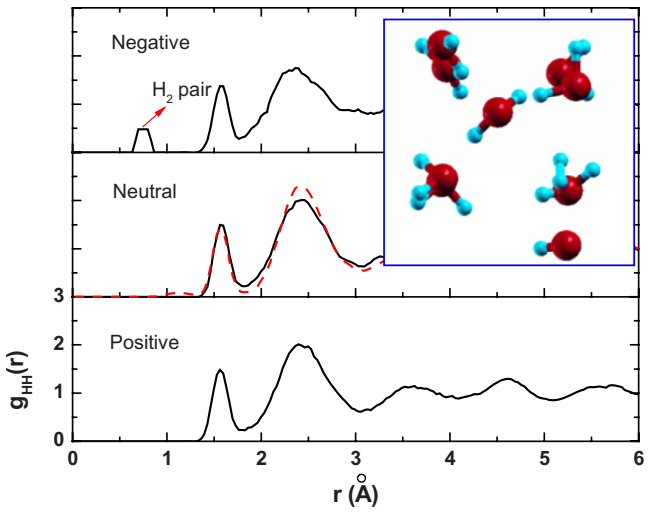


FIG. 3. (Color online) Calculated HH pair distribution in three different environments (electron rich, neutral, and electron deficient) for $NH_3$-like defect model. The inset is a snapshot of the local structure taken from the MD trajectory (O in red, H in blue). The upper panel and the inset clearly show the formation of $H_2$. In the neutral environment, there is an unpaired electron, therefore additional spin-polarized calculations were performed. The resulting H-H RDF (red dashed line, middle panel) shows a very small and broad distribution at 1.2 Å, which is due to a mobile H radical.

with the observed splitting of ~70 $cm^{-1}$. Incidentally, the calculated H-H vibration of free $H_2$ lies between the vibrons of D and in-plane defects as observed in the experiment.[12] Moreover, the predicted frequency shift of the H-H vibron of the in-plane defect from a free molecule of 102 $cm^{-1}$ may be related to the observed shift of ~60 $cm^{-1}$. The formation of $H_2$ can be represented by $[H_2O\cdots H-OH_2]+e^- \rightarrow H_2+H_2O+OH^-$. This scheme is consistent with that suggested from experiments.[14,16] The source of the electron is likely the result of Auger processes. These excess electrons migrate through the H-bonded network in the crystal until they encounter H· radical defect sites where they become trapped and facilitate the dissociation of water forming a $H_2$ molecule and an $OH^-$ ion.

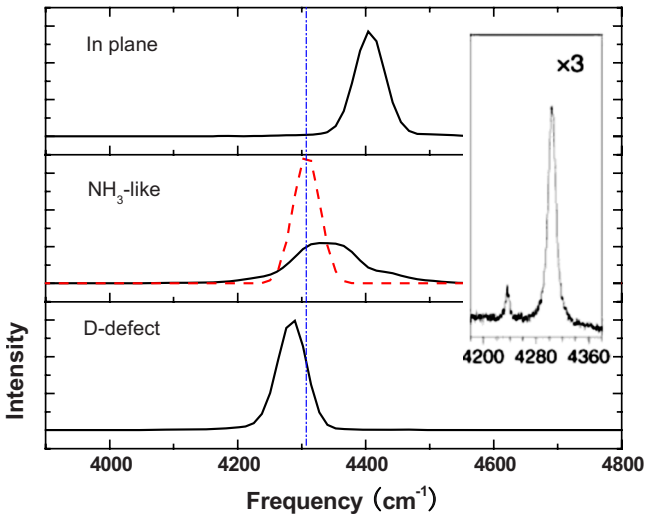


FIG. 4. (Color online) Calculated power spectra of $H_2$ of the three H· defect models in electron-rich environment. From bottom to top, the panels are models with D, $NH_3$-like, and in-plane defects. The calculated spectrum for an isolated $H_2$ is shown in the middle panel for comparison (red dashed line). The straight blue dashed line indicates the frequency of an isolated $H_2$. The inset is the experiment result (Ref. 12). All frequency calculations employed a time step of 2.5 a.u. and a fictitious electron mass of 50 a.u.

### C. Formation of $H_2O_2$ and $O_2$

Next, the interaction of an OH· defect with the environment is studied. As mentioned above, the OH· defect model is generated from the ice VII structure by removing a H atom. The calculated OO RDFs for this model in neutral, positive (hole-electron deficient), and negative (electron rich) environments are compared in Fig. 5. It is found that at the presence of a valence hole (+1*e*), a $H_2O_2$ species with an O-O bond length of 1.49 Å was formed. The OO distance can be compared to the observed 1.45 Å in molecular $H_2O_2$.[34] To confirm that this is indeed molecular $H_2O_2$, the temporal evolution of the H-O-O valance and H-O-O-H dihedral angles was monitored for 2 ps. The average valence and dihedral angles of 101.3° and 98.9° compare very well with that observed in solid $H_2O_2$ of 101.9° and 90.2°. The formation of $H_2O_2$ can be represented by $[H_2O\cdots OH]+hole^+ \rightarrow H_2O_2+H^+$. Analysis of the MD trajectory shows that the $H^+$ is fluxional and fluctuates between water molecules. The positive valence hole required for this process can be created by a screening process where a valence electron is cascaded to fill the core hole after irradiation.[18] It is noteworthy that no O-O bond was found when the OH· radical defect model is in a neutral or electron-rich environment.

Encouraged by the observation of the formation of $H_2O_2$ by a single OH radical defect at the presence of a valence hole, we examine a model with two adjacent OH radicals by removing two H sites bonded to two nearest-neighbor oxygen atoms at the presence of two valence holes (highly electron deficient). The spontaneous formation of $O_2$ (O-O bond length 1.29 Å) was observed (Fig. 5). To take proper account of the triplet state of molecular $O_2$, an additional MD simulation with spin polarization was performed. The $O_2$ bond length is found to be 1.26 Å, which is identical to the calculated value for an isolated $O_2$ and compares well to the observed distance in the condensed phase of ~1.21 Å.[34] The calculated O-O vibrational frequencies are ~1208 $cm^{-1}$, both for the $O_2$ in ice VII and the isolated $O_2$. The formation of a free $O_2$ is also confirmed from the inspection of the MD trajectory. The formation of $O_2$ in the model consisting of two defects (or two H vacancies) with two valence holes can be represented by $[HO\cdots OH]+2hole^+ \rightarrow O_2+2H^+$. Although the production of $O_2$ can be realized in such a model, in reality the probability for the occurrence of two adjacent OH· radicals in a highly electron-deficient environment is expected to be very low. Therefore the formation of $H_2O_2$ as an intermediate product, which eventually transforms into $O_2$, is a more plausible mechanism. Many experiments have already shown that $H_2O_2$ can transform into $H_2O$ and $O_2$ at a similar temperature and pressure range.[34]

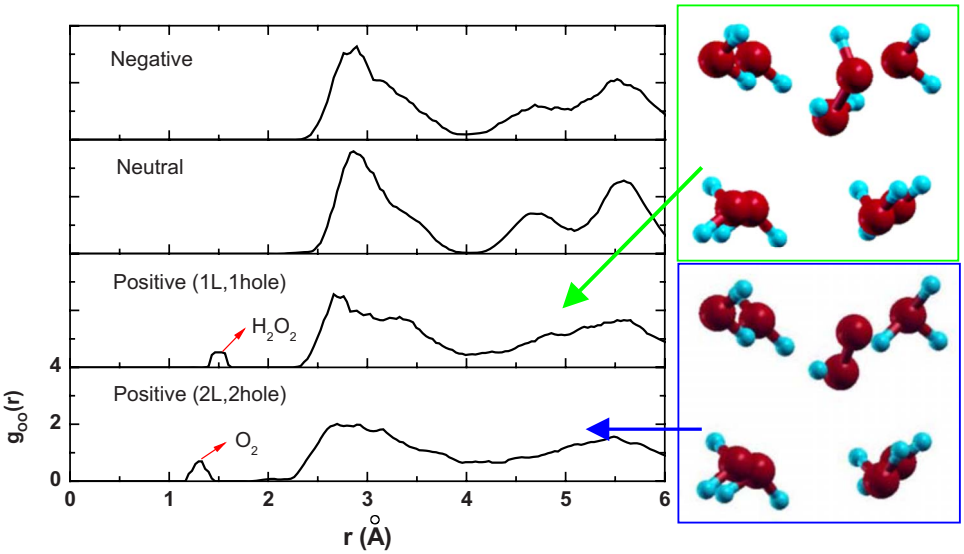


FIG. 5. (Color online) Calculated OO pair distribution under three different environments (neutral, electron rich, and electron deficient) for the configuration with an OH· defect. The bottom panel is the result from a model with two adjacent OH· defects in a two-hole (highly electron deficient) environment. The right panels beside are snapshots taken from MD trajectories, showing the local environment (O in red, H in blue). The panels in blue frame (lower-right) and green frame (upper-right) correspond to configurations with two OH· defects under a highly electron-deficient (two hole) environment and one OH· defect under electron-deficient (one hole) environment, respectively. The bottom two panels clearly show the formation of $H_2O_2$ and $O_2$.

MD calculations were performed for an ice VII model with two adjacent OH radicals under neutral and with one valence (positive) hole. In the neutral system, due to the close proximity of the two OH·, a $H_2O_2$ with O-O bond length of 1.49 Å is formed. The formation process can be represented by $[HO\cdots OH]\rightarrow H_2O_2$. At the presence of a valence hole, an "$O_2$" with a O-O bond distance of 1.37 Å is found. This molecule is attached to a H atom most of the time suggesting a $HO_2$ species. There is no reported O-O distance for $HO_2$, but $HO_2$ has been detected in experiments.[15,21] The formation of $HO_2$ can be described by $[HO\cdots OH]+\text{hole}^+\rightarrow HO_2+H^+$. In both $HO_2$ and $H_2O_2$, no further reaction was found within the time of the simulation (~10 ps). The formation of $H_2O_2$ (and $HO_2$) in the sample with two H vacancies provides additional support for the idea that the $H_2O_2$ (and $HO_2$) may serve as precursor(s) of $O_2$. At this point, we caution that an accurate estimate of the charged states, particularly on odd electron systems, in density-functional theory (DFT) might require the consideration of self-interaction correction.[23,35] Notwithstanding, the formation of closed-shell molecular $O_2$, $H_2O_2$, and $H_2$ are likely not seriously affected.

### D. Effects of pressure

The mechanisms proposed above are based on secondary processes where H· and OH· defects interact with the environment created after core ionization. The amount of $H_2$ and $O_2$ formed depends on the frequency of such interactions. This underlies the importance of the pressure effect. Previous experiments under ambient pressure showed $H_2O_2$ and $O_2$ forms readily after x-ray irradiation.[15,20,21] In ice VII, it was observed that the formation of the molecular species is dependent on the pressure: while only a very small amount of $O_2$ was found below 3 GPa, substantial decomposition of water was observed only above ~9 GPa. We believe that the increased number of defects and their mobility at high pressure[1,3,36–42] can explain this observation. This suggestion is supported by spectroscopic and electrical conductance measurements.[1,3,36,37,41] Experimentally it is shown that the energy barrier on the formation of protonic (radical) defects in ice decreases with increasing pressure.[1,3,36,41] The mobility of defects also increases with pressure from dielectric measurements.[37] From theoretical calculations, Benoit *et al.*[39] have shown that substantial protonic defects in dynamically disordered ice VII exist at high pressure. Theoretical calculations have also shown that the energy barrier for proton transfer decreases one order of magnitude in cationic oligomers of water,[42] when the OO distance decreases from 2.95 to 2.64 Å. These distances correspond to pressure of ~2 and ~17 GPa in ice VII, respectively. Therefore, it is reasonable to suggest that due to the increased number and mobility of defects with pressure, the probability of encountering the environments favoring the formation of $O_2$ and $H_2$ as described here will increase substantially and facilitate the dissociation of water.

## IV. SUMMARY

In summary, from first-principles molecular-dynamics calculations, several possible mechanisms for the dissociation of dense ice (phase VII) into molecular $H_2$ and $O_2$ by the irradiation of x ray are revealed. It has been established that irradiation can lead to the formation of H defects.[17] The

results reported here highlight the importance of the interactions of defect sites with electrons or holes produced by the irradiation process.

The calculations were performed at the Westgrid facilities funded by the Canada Foundation of Innovation. We thank J. L. Kuo for providing the initial ice VII structures used in this study. Y.L. wishes to thank S. Scandolo for valuable discussions.

[1] V. F. Petrenko and R. W. Whitworth, *Physics of Ice* (Oxford, New York, 1999).
[2] P. W. Bridgman, J. Chem. Phys. **5**, 964 (1937).
[3] G. E. Walrafen, M. Abebe, F. A. Mauer, S. Block, G. J. Piermarini and R. Munro, J. Chem. Phys. **77**, 2166 (1982).
[4] W. F. Kuhs, J. L. Finney, C. Vettier, and D. V. Bliss, J. Chem. Phys. **81**, 3612 (1984).
[5] R. J. Nelmes, J. S. Loveday, W. G. Marshall, G. Hamel, J. M. Besson, and S. Klotz, Phys. Rev. Lett. **81**, 2719 (1998).
[6] A. F. Goncharov, V. V. Struzhkin, M. S. Somayazulu, R. J. Hemley, and H. K. Mao, Science **273**, 218 (1996).
[7] M. Bernasconi, P. L. Silvestrelli, and M. Parrinello, Phys. Rev. Lett. **81**, 1235 (1998).
[8] A. F. Goncharov, V. V. Struzhkin, H. K. Mao, and R. J. Hemley, Phys. Rev. Lett. **83**, 1998 (1999).
[9] C. Cavazzoni, G. L. Chiarotti, S. Scandolo, E. Tosatti, M. Bernasconi, and M. Parrinello, Science **283**, 44 (1999).
[10] A. F. Goncharov, N. Goldman, L. E. Fried, J. C. Crowhurst, I. Feng W. Kuo, C. J. Mundy, and J. M. Zaug, Phys. Rev. Lett. **94**, 125508 (2005).
[11] P. Loubeyre, R. LeToullec, E. Wolanin, M. Hanfland, and D. Hausermann, Nature (London) **397**, 503 (1999).
[12] W. L. Mao, H.-K. Mao, Y. Meng, P. J. Eng, M. Y. Hu, P. Chow, Y. Q. Cai, J. Shu, and R. J. Hemley, Science **314**, 636 (2006).
[13] C. J. Pickard and R. J. Needs, J. Chem. Phys. **127**, 244503 (2007).
[14] T. W. Marin, K. Takahashi, C. D. Jonah, S. D. Chemerisov, and D. M. Bartels, J. Phys. Chem. A **111**, 11540 (2007).
[15] C. Laffon, S. Lacombe, F. Bournel, and Ph. Parent, J. Chem. Phys. **125**, 204714 (2006).
[16] J. A. LaVerne and S. M. Pimblott, J. Phys. Chem. A **104**, 9820 (2000).
[17] B. Brena, D. Nordlund, M. Odelius, H. Ogasawara, A. Nilsson, and L. G. M. Pettersson, Phys. Rev. Lett. **93**, 148302 (2004).
[18] D. Nordlund, H. Ogasawara, H. Bluhm, O. Takahashi, M. Odelius, M. Nagasono, L. G. M. Pettersson, and A. Nilsson, Phys. Rev. Lett. **99**, 217406 (2007).
[19] N. Tîmneanu, C. Caleman, J. Hajdu, and D. van der Spoel, Chem. Phys. **299**, 277 (2004).
[20] G. A. Grieves and T. M. Orlando, Surf. Sci. **593**, 180 (2005).
[21] M. T. Sieger, W. C. Simpson, and T. M. Orlando, Nature (London) **394**, 554 (1998).
[22] K. S. Kim, I. Park, S. Lee, K. Cho, J. Y. Lee, J. Kim, and J. D. Joannopoulos, Phys. Rev. Lett. **76**, 956 (1996).
[23] F. Baletto, C. Cavazzoni, and S. Scandolo, Phys. Rev. Lett. **95**, 176801 (2005).
[24] C. S. Liu, N. Kioussis, S. G. Demos, and H. B. Radousky, Phys. Rev. Lett. **91**, 015505 (2003).
[25] R. Car and M. Parrinello, Phys. Rev. Lett. **55**, 2471 (1985).
[26] J. L. Kuo and M. L. Klein, J. Phys. Chem. B **108**, 19634 (2004).
[27] S. Nosé, Mol. Phys. **52**, 255 (1984).
[28] S. Baroni, A. Dal Corso, S. de Gironcoli, P. Giannozzi, C. Cavazzoni, G. Ballabio, S. Scandolo, G. Chiarotti, P. Focher, A. Pasquarello, K. Laasonen, A. Trave, R. Car, N. Marzari, and A. Kokalj, http://www.quantum-espresso.org.
[29] N. Troullier and J. L. Martins, Phys. Rev. B **43**, 1993 (1991).
[30] A. D. Becke, Phys. Rev. A **38**, 3098 (1988); C. Lee, W. Yang, and R. G. Parr, Phys. Rev. B **37**, 785 (1988).
[31] L. Kleinman and D. M. Bylander, Phys. Rev. Lett. **48**, 1425 (1982).
[32] D. Prendergast and G. Galli, Phys. Rev. Lett. **96**, 215502 (2006).
[33] B. G. Johnson, P. M. W. Gill, and J. A. Pople, J. Chem. Phys. **98**, 5612 (1993). The calculated value is 1.22 Å, if PBE functional was employed.
[34] H. Cynn, C.-S. Yoo, and S. A. Sheffeield, J. Chem. Phys. **110**, 6836 (1999).
[35] M. d'Avezac, M. Calandra, and F. Mauri, Phys. Rev. B **71**, 205210 (2005).
[36] D. D. Klug and E. Whalley, J. Chem. Phys. **81**, 1220 (1984).
[37] P. V. Hobbs, *Ice Physics* (Clarendon, Oxford, 1974).
[38] M. Benoit, D. Marx, and M. Parrinello, Nature (London) **392**, 258 (1998).
[39] M. Benoit, A. H. Romero, and D. Marx, Phys. Rev. Lett. **89**, 145501 (2002).
[40] E. R. Lippincott and R. Schroeder, J. Chem. Phys. **23**, 1099 (1955).
[41] H. J. Bakker and H.-K. Nienhuys, Science **297**, 587 (2002).
[42] S. Scheiner, J. Am. Chem. Soc. **103**, 315 (1981).